J. Fluid Mech. (1995), *vol.* 295, *pp.* 1–22

Steady flow past a circular cylinder coated with magnetic fluid: flow structure, drag reduction and coating deformation

By MIKHAIL S. KRAKOV[1] AND SHINICHI KAMIYAMA[2]

[1] Heat and Power Department, Byelorussian State Polytechnic Academy, Minsk 220027, Republic of Belarus

[2] Institute of Fluid Science, Tohoku University, Sendai 980, Japan

(Received 26 May 1994)

The present study deals with the influence of a magnetic-fluid coating, held onto a circular cylinder surface by a magnetic field, on the viscous fluid flow structure round the cylinder in the Reynolds number range of 1–100. The influence of the coating thickness, magnetic fluid viscosity, and Reynolds number on flow separation and drag reduction is determined. The interface shape of the magnetic fluid coating and its behaviour, depending on the flow parameters, are also established.

1. Introduction

It is well known that the flow structure near a solid body surface is determined by a balance of a viscous friction force and a pressure drop. For flow past a finite solid body, the flow to the rear of the body decelerates due to viscous friction. Then, an adverse pressure gradient develops in the flow direction, and flow separation is possible.

As the pressure gradient in the fluid flow near the solid surface is determined by viscous friction and the solid surface shape, there are two ways to modify the flow structure near the body: either changing the body shape or varying the viscous friction on its surface.

The first is well known and is not the subject of the present study. The second may be done in different ways, e.g. by heating a surface or by inserting gas bubbles or low-viscosity fluid drops into the fluid surface layer. On the other hand, at the beginning of the century a procedure was proposed to modify the flow structure by applying a low-viscosity fluid film (Isaak & Speed 1906) on the body surface. Because of the small fluid-film viscosity, energy dissipation by friction sharply decreases in the wall region, and the pressure gradient remains favourable everywhere. This means that the low-viscosity fluid film on the body surface hinders flow separation and reduces drag, too.

The drawback of this procedure for affecting the flow structure is that the low-viscosity fluid film is easily separated from the body surface by the flow. Therefore, the present study is concerned with a low-viscosity fluid coating of the body surface which possesses magnetic properties and is kept on the surface under a magnetic field. Such a fluid is called a magnetic fluid.

A magnetic fluid is an artificial medium synthesized in the mid-60s and represents a colloid solution of small (of the order of 10 nm) magnetic particles coated with a surfactant layer. The surfactant prevents the coalescence of particles which are attracted to each other due to magnetic interaction. As their size is small the particles

are subject to Brownian motion which provides both a uniform particle distribution within the fluid volume and energy and momentum transfer from an external magnetic field to the carrying fluid. These factors determine the main properties of magnetic fluids: these are stable uniform fluids which are able to preserve fluidity and, at the same time, to be magnetized under an applied magnetic field (Rosensweig 1985; Kamiyama & Shimoiizaka 1985; Bashtovoi, Berkovsky & Vislovich 1988; Berkovsky, Medvedev & Krakov 1993).

This ability of magnetic fluids to be magnetized allows a layer of such a fluid to be held on the body surface under a magnetic field. If the viscosity of such a coating is rather small, then as is usual for a low-viscous fluid film, this will affect the flow structure and drag. In the present study, this problem is analysed using the example of circular magnetic-fluid-coated cylinder.

2. Governing equations

A magnetic fluid is a complex system comprising fluid-carrying media, magnetic particles, and surfactant which interact with each other and with an external magnetic field. Generally speaking, the behaviour of such a system depends in an intricate manner on its interior structure, interparticle interactions and interactions between particles and the external magnetic field, the shear rate during fluid flow, and the magnitude of an external magnetic field. Numerous mathematical models for the behaviour of such a system allow the basic factors influencing a magnetic fluid motion under an external magnetic field to be specified and the main effects of the external field action upon the fluid to be revealed. Among studies of phenomena bound up with the free surface of a magnetic fluid and its flow due to external factors, of most use is a model which is simple and relevant to physical experiments, does not include the interior fluid structure, and assumes the fluid to be superparamagnetic. This model (Neuringer & Rosensweig 1964) is based on a stress tensor which is the sum of viscous fluid and Maxwell's magnetic field stress tensors in a magnetizing medium. The fluid in this case is considered non-conducting, and magnetization to be proportional to the fluid density (i.e. magnetic particle concentration). This yields Maxwell's stress tensor in the form $T_{ik} = H_i B_k - \delta_{ik}\mu_0 H^2/2$ (Landau, Lifshitz & Pitaevskii 1984).

A system of equations for incompressible fluid motion in this case is of the form

$$\left.\begin{aligned} \rho\left(\frac{\partial v_i}{\partial t} + v_k \frac{\partial v_i}{\partial x_k}\right) &= \frac{\partial \sigma_{ik}}{\partial x_k} + F_i, \\ \frac{\partial v_k}{\partial x_k} &= 0, \end{aligned}\right\} \tag{2.1}$$

where F_i is the body force, and the stress tensor σ_{ik} has the form

$$\sigma_{ik} = -p\delta_{ik} + \sigma'_{ik} + T_{ik},$$

$$\sigma'_{ik} = \eta\left(\frac{\partial v_i}{\partial x_k} + \frac{\partial v_k}{\partial x_i}\right).$$

Also, the Maxwell equations must be satisfied, which for a non-conducting medium and steady magnetic fields are of the form

$$\nabla \times \boldsymbol{H} = 0; \quad \nabla \cdot \boldsymbol{B} = 0, \tag{2.2}$$

where $\boldsymbol{H}$ is the magnetic field intensity and $\boldsymbol{B}$ is its induction. In this situation, the equation of state for a magnetic fluid is of the following form:

$$\boldsymbol{M} = (M/H)\,\boldsymbol{H}; \quad M = M(\rho, H, T).$$

At the boundary of a fluid-occupied volume the ordinary hydrodynamic conditions must be satisfied: no-slip on solid surfaces, equality of velocities, and tangential and normal stresses at the interface of the two fluids. The last condition in the general case is of the form

$$(\sigma_{ik}^{(1)} - \sigma_{ik}^{(2)})\,n_k = \alpha\left(\frac{1}{R_1} + \frac{1}{R_2}\right)\delta_{ik}\,n_k + \frac{\partial \alpha}{\partial x_i}, \tag{2.3}$$

where α is the surface tension, and R_1 and R_2 are the radii of the surface curvature.

In addition, at the interface of two media with different magnetic properties the continuity conditions for a normal induction component and a tangential magnetic field intensity component must be obeyed:

$$(\boldsymbol{B}^{(1)} - \boldsymbol{B}^{(2)}) \cdot \boldsymbol{n} = 0; \quad (\boldsymbol{H}^{(1)} - \boldsymbol{H}^{(2)}) \times \boldsymbol{n} = 0. \tag{2.4}$$

Equation (2.1) differs from the ordinary Navier–Stokes equation only in the form of the stress tensor which incorporates the Maxwell stress tensor, T_{ik}, of a magnetic field. This difference yields an additional body force $\mu_0 M \nabla H$. This force is potential, does not depend on fluid velocity, and results only in a pressure re-distribution in the fluid volume. In an infinite volume, the available force $\mu_0 M \nabla H$ does not affect the fluid motion. However, if the magnetic-fluid volume is finite, then the force $\mu_0 M \nabla H$ defines its position in space and the free surface shape. Because under the magnetic force $\mu_0 M \nabla H$ a magnetic fluid is pulled into a region of a strong magnetic field, it proves possible to produce magnetic-fluid coatings using a system of permanent magnets on solid surfaces. When permanent magnets are used, the magnitude of this force exceeds the fluid weight a dozen times, thus holding the magnetic fluid coating reliably on the solid surface.

Thus, the magnetic force $\mu_0 M \nabla H$ defines the position and the surface shape of the magnetic-fluid volume, thereby influencing the flow structure of a non-magnetic fluid around the body. This means that determining the flow structure near a magnetic-fluid coating, and the previously unknown coating shape and flow inside it, is a self-conjugate problem.

3. Creation of a circular coating on a cylinder surface

If an immovable magnetic fluid has a free surface, then the pressure distribution on it is governed by the equation

$$\nabla p = \mu_0 M \nabla H. \tag{3.1}$$

From (3.1) it follows that a surface with a constant pressure $p(x, y, z) = \text{const}$ is the same as one under a constant magnetic field with an intensity $H(x, y, z) = \text{const}$. It is known that, for a immovable fluid, a constant-pressure surface coincides with a free one. Thus, the immovable magnetic fluid surface coincides with the constant-magnetic-field one.

This means that for a circular magnetic-fluid coating to be created on a cylinder surface, a magnetic field possessing axial symmetry and decreasing at a distance from the cylinder must be induced. The latter is necessary for the volume magnetic force $\mu_0 M \nabla H$ to be directed to the symmetry axis and the magnetic-fluid coating to be held on the cylinder surface.

There are two sources that induce a magnetic field obeying the above conditions. An electric current I flowing along the cylinder induces a magnetic field which in cylindrical (r, θ, z)-coordinates is of the form

$$H = \{0; I/2\pi r; 0\}. \tag{3.2}$$

Such a magnetic field does not depend on the angle θ, and the magnetic force $\mu_0 M \nabla H$ has a radial component only. If a cylinder is uniformly magnetized normal to the axis, then its magnetic field has the following structure:

$$\boldsymbol{H} = \left\{ \frac{M_I R^2}{2r^2} \cos\theta; \frac{M_I R^2}{2r^2} \sin\theta; 0 \right\}, \tag{3.3}$$

where R is the cylinder radius and M_I is the saturation magnetization of the material from which the cylinder is made. In this case, the magnitude of the field $H = M_I R^2/2r^2$ also does not depend on the angle θ and the free magnetic fluid surface has the shape of a circular cylinder.

Of significance is the problem of the stability of a cylindrical magnetic-fluid surface. There are at least two causes of instability. First, the cylindrical surface of the fluid is unstable due to capillary forces (Rayleigh 1878). However, the volume force $\mu_0 M \nabla H$ normal to the symmetry axis is able to suppress this mode of instability (Bashtovoi & Krakov 1978). The magnetic field influence is characterized by a dimensionless magnetic Bond number $Bo_m = \mu_0 M \nabla H h^2/\alpha$ being the magnetostatic-to-capillary pressure ratio. In Bashtovoi & Krakov (1978), it is shown that for values of the magnetic Bond number greater than unity ($Bo_m > 1$, in this case h is the radius of an interface a) the cylindrical surface of a magnetic fluid is stable.

For a conductor with a current $I = 10$ A and 2 mm radius the magnetic field ($H = I/2\pi r \approx 0.8$ kA m^{-1}) is not high and the linear magnetization law $M = \chi H$ may be used for a magnetic fluid. $\chi = 5$ and $\sigma = 10^{-2}$ N m^{-1} are typical values for the coefficients of magnetic susceptibility χ and surface tension σ. For these values of the parameters the magnetic Bond number is equal to $Bo_m \approx 3$, and the cylindrical magnetic fluid surface is stable.

If the cylinder is a magnet magnetized transverse to the axis, then for the above-mentioned physical parameters the magnetic Bond number is greater than unity with a cylinder saturation magnetization of $M_I > 1.2$ kA m^{-1}. As $M_I \approx 100$ kA m^{-1} is a characteristic magnitude of the magnetization of permanent magnets, in this case the magnetic Bond number greatly exceeds unity, and the cylindrical surface must be stable.

However, magnetic fields are characterized by specific modes of free surface instability developing under magnetic fields. So, a magnetic field normal to a free magnetic-fluid surface and greater than some critical value gives rise to cone-shaped peaks on this surface (Cowley & Rosensweig 1967). The stability of the free magnetic-fluid surface is detailed in Bashtovoi *et al.* (1988) where it is also shown that the instability starts if the value of the surface instability criterion $Si = \mu_0 M_n^2/(f\alpha)^{1/2}$ is greater than 4, where f is the body force density ($f = \rho g$ for gravitational forces) and M_n is the magnetization vector component normal to the free magnetic fluid surface.

Like the current conductor, the magnetic field (3.2) has an azimuthal component only, the normal magnetization component M_n equals zero, and the magnetic fluid surface is stable. With the cylindrical magnet, the situation is more severe as $H_r \neq 0$. In this case, $f = \mu_0 M \nabla H$ and the value of the Si criterion is affected by the fluid magnetization law and by the value of the cylinder magnetization. In regard to a

magnet with a magnetization $M_I = 10$ kA m^{-1}, the linear fluid magnetization law may be used, and then we have $Si \approx 20$ for the above values of the physical parameters, i.e. in the field of a relatively weak permanent magnet the cylindrical surface is unstable. Since the fluid magnetization grows more weakly than the magnetic field that magnetizes it, the case may be opposite for rather strong magnets. Indeed, for a cylinder with a magnetization of 200 kA m^{-1}, the magnetic-fluid magnetization may be considered constant. For $M_n = 10$ kA m^{-1} we shall obtain $Si \approx 1.1$. This provides the stability of the cylindrical surface of the magnetic fluid.

Thus, through the use of a current flowing along the cylinder or due to the magnetic properties of the material from which a cylinder is made, a magnetic-fluid coating its surface may be created, also having a cylindrical shape. Such a coating is stable and is held on the magnetic surface by a non-uniform magnetic field.

4. Flow structure change and drag reduction by magnetic-fluid coating

4.1. *Small Reynolds numbers: analytical investigation*

Let us consider flow near a magnetic-fluid-coated cylinder (figure 1) by making simplifying assumptions. The interface between the magnetic fluid and the outer flow is affected by magnetic and hydrodynamic forces. In the present section, the magnetic forces are assumed to be far greater than the hydrodynamic ones. This means that the surface shape of the magnetic fluid coating is determined by the magnetic forces alone and is a circular cylinder. This situation essentially simplifies the problem since boundary conditions can be written at a fixed interface which is known beforehand. In addition, let us simplify the equation of motion. First, let us restrict our consideration to steady flow past a cylinder. Moreover, for small flow velocities the inertia terms in the equation of motion (2.1) are small and can be modified. With a magnetic fluid moving near the cylinder, these may be neglected, i.e. Stokes' approximation can be employed. Oseen's approximation can be used for the outer fluid flow, according to which the inertia term $(\boldsymbol{v}\cdot\nabla)\boldsymbol{v}$ can be replaced by $(\boldsymbol{U}\cdot\nabla)\boldsymbol{v}$ where $\boldsymbol{U}$ is the flow velocity at infinite distance from the cylinder. Simultaneous use of Stokes' and Oseen's approximations is possible because these have the same accuracy near the cylinder surface (Lamb 1932). Then the stated problem is governed by the equations

$$\left.\begin{gathered}\nabla p_2^0 = \eta_2 \Delta \boldsymbol{v}_2, \quad p_2^0 = p_2 + \int_0^H \mu_0 M(H')\,\mathrm{d}H', \\ \rho_1(\boldsymbol{U}\cdot\nabla)\boldsymbol{v}_1 = -\nabla p_1 + \eta_1 \Delta \boldsymbol{v}_1, \\ \nabla\cdot\boldsymbol{v}_1 = 0; \quad \nabla\cdot\boldsymbol{v}_2 = 0,\end{gathered}\right\} \tag{4.1}$$

where subscripts 1 and 2 refer to the outer flow and the magnetic fluid, respectively, and p_2^0 is the magnetic fluid pressure ($\nabla p_2^0 = \nabla p_2 + \mu_0 M \nabla H$).

The fluid motion must obey the following boundary conditions: the no-slip condition for the solid surface

$$\boldsymbol{v} = 0; \quad r = R; \tag{4.2}$$

equality conditions for velocities and shear stresses at the interface of the magnetic fluid and outer flow

$$\left.\begin{gathered}v_{1r} = v_{2r} = 0; \quad v_{1\theta} = v_{2\theta}, \\ \eta_1\left(\frac{1}{a}\frac{\partial v_{1r}}{\partial\theta} + \frac{\partial v_{1\theta}}{\partial r} - \frac{v_{1\theta}}{a}\right) = \eta_2\left(\frac{1}{a}\frac{\partial v_{2r}}{\partial\theta} + \frac{\partial v_{2\theta}}{\partial r} - \frac{v_{2\theta}}{a}\right),\end{gathered}\right\} \quad r = a; \tag{4.3}$$

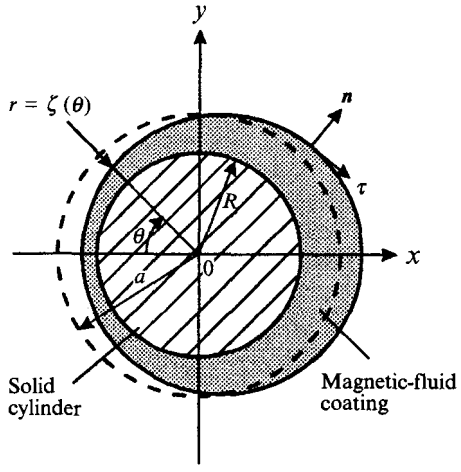

FIGURE 1. Problem geometry.

and the condition of uniform flow at infinite distance from the cylinder

$$v_1 = \{U\cos\theta; -U\sin\theta; 0\}, \quad p_1 = p_0, \quad r \to \infty. \tag{4.4}$$

A general solution to Oseen's equation is well known (Lamb 1932), and finding a solution to Stokes' equation involves no difficulty. With these solutions obeying boundary conditions (4.2)–(4.4) the fluid velocity and pressure distributions can be written as

$$v_{1r} = \frac{U\cos\theta}{D}\left\{\frac{1}{2}\frac{\eta_1}{\eta_2}F\ln r' - A\left[\ln r' + \frac{1}{2}\left(1-\frac{1}{r'^2}\right)\right]\right\}, \tag{4.5a}$$

$$v_{1\theta} = \frac{U\sin\theta}{D}\left\{\frac{1}{2}\frac{\eta_1}{\eta_2}F(\ln r'+1) + A\left[\ln r' + \frac{1}{2}\left(1-\frac{1}{r'^2}\right)\right]\right\}, \tag{4.5b}$$

$$v_{2r} = \frac{1}{2}\frac{\eta_1}{\eta_2}\frac{\delta^2}{D}U\cos\theta\left\{\ln r'(1-\delta^2)\left(1-\frac{r'^2}{\delta^2}\right) - 2\ln\frac{r'}{\delta}\ln\delta(1-r'^2)\right\}, \tag{4.5c}$$

$$v_{2\theta} = -\frac{1}{2}\frac{\eta_1}{\eta_2}\frac{\delta^2}{D}U\sin\theta\left\{(1+\ln r')(1-\delta^2) + 2\ln\delta\left[1+\ln\left(\frac{r'}{\delta}\right)\right]\right.$$
$$\left. -\left(\frac{r'}{\delta}\right)^2\left[2\delta^2\ln\delta\left(1+3\ln\frac{r'}{\delta}\right) + (1-\delta^2)(1+3\ln r')\right]\right\}, \tag{4.5d}$$

$$p_1 = p_2 + \frac{\eta_1 U\cos\theta}{Dr}\left(2A + \frac{\eta_1}{\eta_2}F\right), \tag{4.5e}$$

$$p_2^0 = \frac{\eta_1 UR}{a^2 D}\cos\theta\left\{-\left(\frac{1}{r'}+7r'\right)(1-\delta^2+2\ln\delta) + 4r'(\delta^2-1)\ln r'\right.$$
$$\left. -8r'\delta^2\ln r'\ln\delta\right\} + p_0 + [p_M(r') - p_M(1/\delta)], \tag{4.5f}$$

where $r' = r/a$ ($r' = 1$ corresponds to the interface, $r' = \delta$ corresponds to the solid surface),

$$p_M(r) = \int_0^H \mu_0 M(H')\,\mathrm{d}H$$

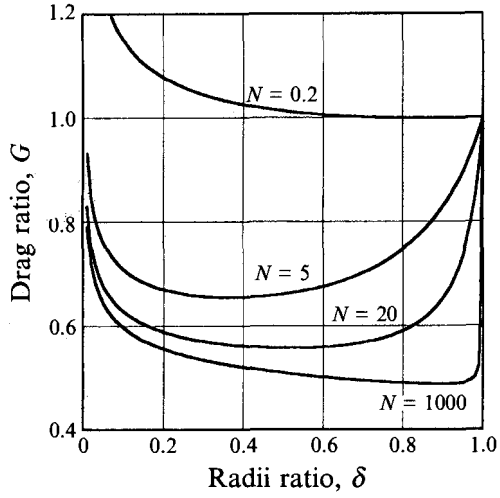

FIGURE 2. Dependence of the drag ratio G on the coating thickness. $\gamma Re/8 = 0.1$.

and the constants entering the above expressions are

$$D = \frac{1}{2}\frac{\eta_1}{\eta_2}\left[\ln\left(\frac{\gamma Re}{8\delta}\right)-1\right]F+\left[\ln\left(\frac{\gamma Re}{8\delta}\right)-\frac{1}{2}\right]A,$$

$$A = 1-\delta^2[1-2\ln\delta(1-\ln\delta)], \quad F = (1-\delta^2)^2-4\delta^2\ln^2\delta,$$

$$\delta = R/a, \quad Re = \rho_1 U2R/\eta_1.$$

Here $\gamma = 1.7811\ldots$ is Maskeroni's constant, $r' = 1$ corresponds to the interface, $r' = \delta$ corresponds to the solid surface.

The drag on a magnetofluid-coated cylinder can be calculated as an integral along the interface from the following expression:

$$W = a\int_0^{2\pi}\left\{\left(-p_1+2\eta_1\frac{\partial v_{1r}}{\partial r}\right)\cos\theta-\eta_1\left(\frac{1}{a}\frac{\partial v_{1r}}{\partial\theta}+\frac{\partial v_{1\theta}}{\partial r}-\frac{v_{2\theta}}{a}\right)\sin\theta\right\}_{r=a}\mathrm{d}\theta$$

$$= W_0\frac{1-2\ln(\gamma Re/8)}{1-2\ln(\gamma Re/8\delta)}\frac{1+NF/(2A)}{1+2\dfrac{NF}{A}\dfrac{1-\ln(\gamma Re/8\delta)}{1-2\ln(\gamma Re/8\delta)}} = W_0 G, \tag{4.6}$$

where $W_0 = 8\pi\eta_1 U/[1-2\ln(\gamma Re/8)]$ is the known Lamb formula for the drag per unit length on an infinite cylinder R in radius, $N = \eta_1/\eta_2$ is the viscosity ratio of two fluids. The quantity G in (4.6) is the ratio of the drag on a magnetic-fluid-coated cylinder to that on an uncoated one and characterizes the variation in cylinder drag when a magnetic fluid coating is applied over the cylinder surface. This quantity depends on a coating thickness, fluid viscosity ratio, and Reynolds number. Figure 2 plots the drag ratio G *vs.* δ at $\gamma Re/8 = 0.1$, with the relative viscosity N taking values of 1000, 20, 5, 0.2. It is seen that for a small coating thickness $G \to 1$ as $\delta \to 1$, i.e. a small thickness coating hardly affects the cylinder drag. As the coating thickness increases, its influence on the cylinder drag depends on the relative viscosity N: for small values of N the drag on the magnetic-fluid-coated cylinder increases, and as the viscosity ratio grows the cylinder drag falls with decreasing δ. This means that a magnetic fluid coating with a small viscosity (large values of N) changes the flow structure and pressure distribution in a such manner that the drag on the coated cylinder becomes smaller than that on the uncoated one.

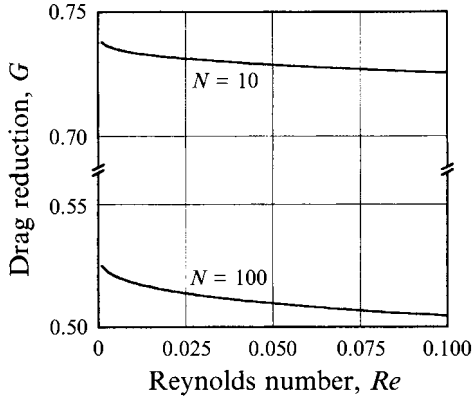

FIGURE 3. Influence of Reynolds number on drag reduction. $\delta = 0.9$.

Figure 3 plots the drag ratio G *vs.* Reynolds number Re at $\delta = 0.9$ and $N = 10$ and $N = 100$. It is seen that with increasing Reynolds number, G decreases, i.e. the effect of applying a coating over the cylinder surface is enhanced. This is, apparently, bound up with different contributions of friction drag and pressure drag to the total drag magnitude.

In fact, there are several factors responsible for the drag change on the cylinder when its surface is coated with a magnetic fluid. First, the coating increases the cylinder cross-section and the pressure drag rises, with consequent growth of the pressure drag coefficient C_{Dp}, defined in the usual way through the cylinder diameter. However, if the magnetic fluid viscosity is small, then flow boundary friction decreases and, accordingly, the friction drag coefficient C_{Df} reduces. The total effect depends on the relationship between these two factors as both they depend on coating thickness.

For a sufficiently small viscosity of the magnetic fluid the situation is possible where the decrease in C_{Df} is greater than the increase in C_{Dp}, so that the total drag coefficient will be smaller than in the case of the uncoated cylinder, as seen in figure 2. But friction makes its main contribution to C_{Df} only at small Reynolds numbers. When the Reynolds number increases, the structure of the flow around the uncoated cylinder becomes more complicated and, as will be exemplified below by figures 4 and 5, applying a low-viscosity coating will result in non-separated flow, i.e. in a considerable C_{Dp} decrease. Therefore, this factor becomes still more important when the Reynolds number increases, thus reducing the coefficient G in figure 3.

4.2. *Moderate Reynolds numbers: numerical simulation*

An analytical study of the problem under consideration is restricted to small Reynolds numbers and gives no possibility of analysing changes in the flow structure, flow separation and pressure distribution when a coating is applied over a cylinder surface under real flow velocity conditions. A detailed study of the influence of the coating on the flow structure and magnetic-fluid-coated cylinder drag has been made numerically. An infinite cylinder has been examined, and the problem has been considered to be two-dimensional. As fluids are assumed incompressible, stream function–vorticity variables has been used

$$\frac{Re}{2} L_i \left(\frac{\partial \psi_i}{\partial y} \frac{\partial \omega_i}{\partial x} - \frac{\partial \psi_i}{\partial x} \frac{\partial \omega_i}{\partial y} \right) = -\Delta \omega_i, \tag{4.7}$$

$$\Delta \psi_i = -\omega_i, \tag{4.8}$$

where the stream function ψ is related to velocity field by $v_x = \partial \psi / \partial y$ and $v_y =$

$-\partial\psi/\partial x$, and the vorticity ω is determined by the relation $\boldsymbol{\omega} = \nabla \times \boldsymbol{v}$. Subscripts $i = 1$ and $i = 2$ refer to the outer flow and magnetic fluid, respectively; $L_i = \nu_i/\nu_1$ is the kinematic viscosity ratio, and the cylinder radius is used as a characteristic dimension.

On the solid cylinder surface, a no-slip condition (4.2) is used as a boundary condition, with uniform flow condition (4.4) at infinity.

At the fluid interface there is another type of physical boundary condition: equality of tangential velocities and shear stresses. These conditions can be written in the form

$$v_{1\tau} = v_{2\tau}, \tag{4.9}$$

$$\sigma_{ik}^{(1)} n_k \tau_i = \sigma_{ik}^{(2)} n_k \tau_i, \tag{4.10}$$

where v_τ is the velocity tangential to the interface, σ_{ik} is the tensor of viscous stresses, $\boldsymbol{n}$ and $\boldsymbol{t}$ are the unit vectors normal and tangential to the line of the interface. The interface is assumed to be fixed and the normal velocity at each point of the interface to be equal to zero.

For the problem to be solved, the finite element method has been adapted, and its formulation for the equation of motion in the stream function–vorticity variables is cited in Krakov (1992) and Kamiyama & Krakov (1993). This method allows a high-accuracy calculation of flow near complex-geometry bodies in the case of multiphase flows because, based on the boundary conditions (4.9) and (4.10), the boundary conditions for vorticity at the fluid interface have been formulated within the framework of this method.

The numerical study is made on a grid composed of 5751 nodes. With the problem symmetry taken into account, a grid is constructed on the half-space $y > 0$. The domain is subdivided into 71 segments by an angle θ, the angle $\Delta\theta$ in the rear part of the cylinder decreases according to a quadratic law. Each line $\theta = \text{const}$ is subdivided into 20 equal pieces inside the magnetic fluid layer. In the domain outside the magnetic-fluid coating, the first piece is chosen equal to the one inside the coating, and the subsequent pieces increase, following a geometric progression, whose denominator is independently chosen such that the last point will be at the external boundary of the design domain. The distance from the cylinder to the flow entrance is chosen equal to 20 (the cylinder radius serves as a characteristic dimension), equal to 100 up to the exit and equal to 40 up to the upper flow boundary. These values are selected so that the boundary conditions at the external boundary of the domain will exert no influence on the computational accuracy. Uniform flow ($\psi = y$) and vorticity-free flow ($\omega = 0$) are taken as the boundary conditions at the external boundary.

Test computations for an uncoated cylinder have shown that over the Reynolds number range $Re = 1$–100 the drag coefficient C_D differs by no more than 2.5% from that calculated in well-known previous papers (Takami & Keller 1969; Dennis & Chang 1970; Fornberg 1980).

The flow structure near a magnetic-fluid-coated cylinder is determined by using three parameters: Reynolds number (Re), cylinder-to-coating radius ratio ($\delta = R/a$), and viscosity ratio ($N = \eta_1/\eta_2$). The problem has been analysed over a broad parameter range: $Re = 1$–100, $N = 1$–1000, $1/\delta = 1$–1.7.

Figure 4 illustrates how the flow behaviour changes with decreasing magnetic-fluid viscosity. If the magnetic-fluid viscosity is comparable with that of the outer fluid ($N = 1$), then flow separation is observed behind the cylinder, and inside the coating the flow consists of two closed cells (figure 4*a*). The boundary between these two cells is always located exactly at the external flow separation angle, as the condition of the equality of tangential velocity $v_{1\tau} = v_{2\tau}$ must be fulfilled on the interface: if the recirculation flow arises in the outer fluid flow and tangential velocity $v_{1\tau}$ changes

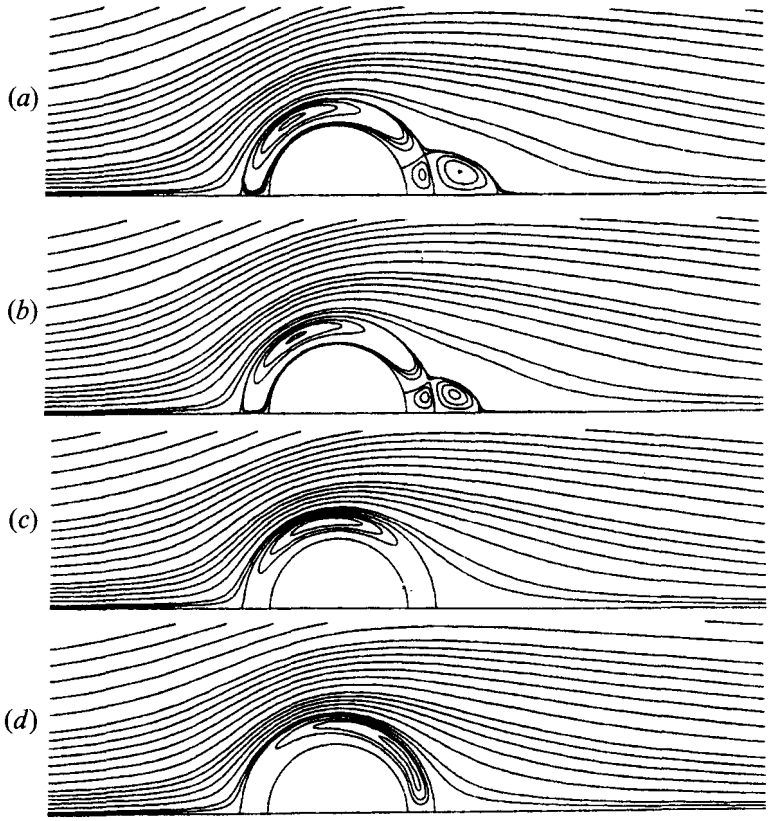

FIGURE 4. Streamlines at different viscosity ratio for $Re = 10$, $1/\delta = 1.4$: (*a*) $N = 1$, (*b*) $N = 10$, (*c*) $N = 100$, (*d*) $N = 1000$.

direction, the corresponding recirculation has to arise in the magnetic fluid coating. As the magnetic-fluid viscosity decreases (i.e. when the parameter N increases) the separation flow region decreases in size (figure 4*b*), eventually completely disappearing (figure 4*c*, *d*). Flow inside the magnetic-fluid layer becomes therewith single-cell, and thus the cell centre is shifted downstream with increasing parameter N. The magnitude of the pressure gradient at the rear part of the cylinder grows and the flow structure approaches that of an ideal fluid.

Even a thin magnetic fluid layer is able to prevent flow separation past a cylinder. Figure 5 shows that for $Re = 10$ flow is non-separated, whereas for an uncoated cylinder, flow separation is seen at $Re \approx 5$. However, increasing the Reynolds number results in the onset of a separated flow region behind the cylinder, whose length is nevertheless smaller than in the case of the uncoated cylinder (figure 5*a*, *b*).

As has been shown in analysing flow at small Reynolds numbers, coating a cylinder with a magnetic-fluid layer not only changes the flow structure but also the drag coefficient C_D. This change is determined by the relationship between two factors: drag growth due to the cylinder cross-section increase because of the coating and reduction due to the low viscosity of the coating. The total effect depends on both the coating thickness (parameter δ) and the magnetic fluid viscosity (parameter N). The flow structure is also determined by the Reynolds number. Therefore, the Reynolds number is the third, no less important, parameter of the problem. Let us examine the influence of these factors upon the value of the coefficient G.

Starting with a Reynolds number around unity, the pressure drag coefficient C_{Dp},

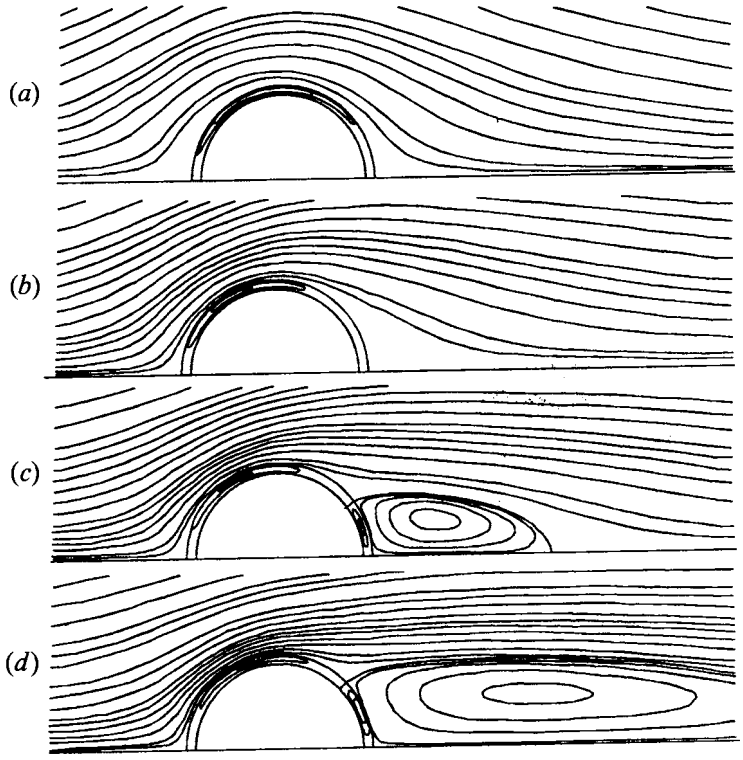

FIGURE 5. The ψ field at different Reynolds number for $N = 100$, $1/\delta = 1.1$. (*a*) $Re = 1$, (*b*) $Re = 10$, (*c*) $Re = 30$, (*d*) $Re = 100$.

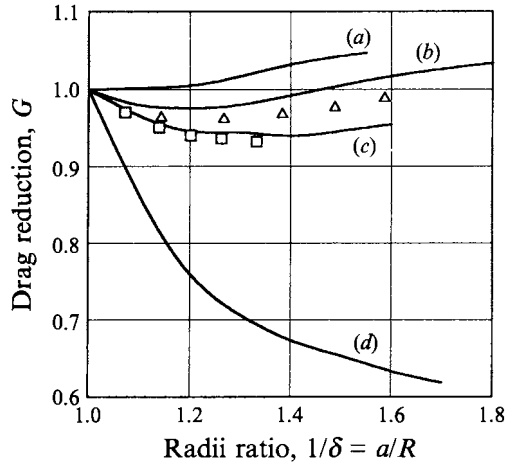

FIGURE 6. Drag ratio G *vs.* coating thickness. $N = 100$, (*a*) $Re = 1$; (*b*) $Re = 10$; (*c*) $Re = 20$; (*d*) $Re = 100$. Experimental data: △, $Re = 7.28$; □, $Re = 17.5$.

dependent mainly on the non-symmetric behaviour of the pressure distribution along the cylinder surface because of flow separation, becomes predominant. This means that with growing Re, the drag reduction coefficient G must fall more quickly than at small Reynolds numbers since, as seen from figures 4 and 5, the magnetic-fluid coating changes the flow structure considerably and, accordingly, the pressure drag coefficient C_{Dp}. These points are clearly illustrated in figure 6, showing the drag reduction

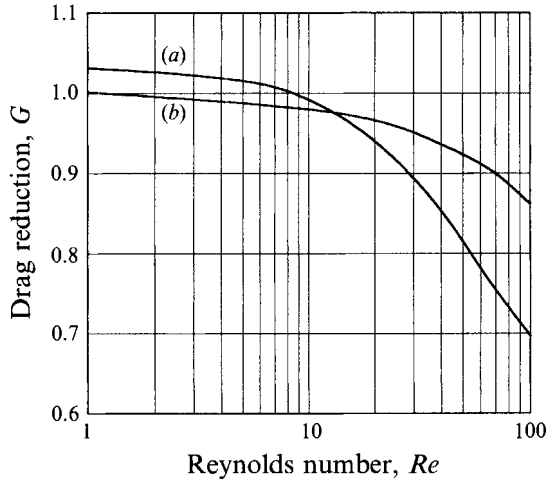

FIGURE 7. Drag ratio G dependence on Reynolds number for $N = 100$ and (*a*) $1/\delta = 1.4$, (*b*) $1/\delta = 1.1$.

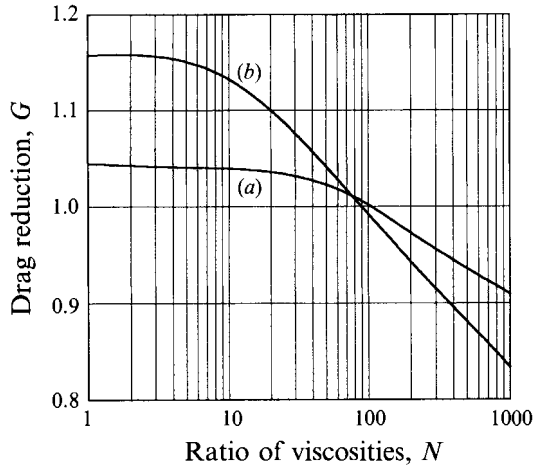

FIGURE 8. Influence of viscosity ratio N on drag ratio. (*a*) $Re = 1$, $1/\delta = 1.1$; (*b*) $Re = 10$, $1/\delta = 1.4$.

coefficient G as a function of coating thickness $1/\delta$ for different values of the Reynolds number.

For $Re = 1$ the curve $G(1/\delta)$ is monotonic in nature: the cylinder drag grows with increasing coating thickness. This suggests that the pressure drag grows with increasing cylinder cross-section more quickly than the friction drag falls, although the viscosity ratio in this case is equal to 100. At large Reynolds numbers, a minimum appears in the curve: with increasing coating thickness, the cylinder drag first falls.

As has already been mentioned, the reason for this fall is the more substantial influence of the coating on the flow structure and, hence, on the pressure drag at high Reynolds numbers. This is illustrated by the curve $G(Re)$ shown in figure 7. Unlike previous data (Polevikov 1986), the relation of G to Re is monotonic.

Although for the data plotted in figures 6 and 7 it is seen that at $Re = 1$ the unequality $G > 1$ is satisfied, it is possible to attain a cylinder drag reduction even for low Reynolds numbers by using a magnetic fluid with lower viscosity. Figure 8

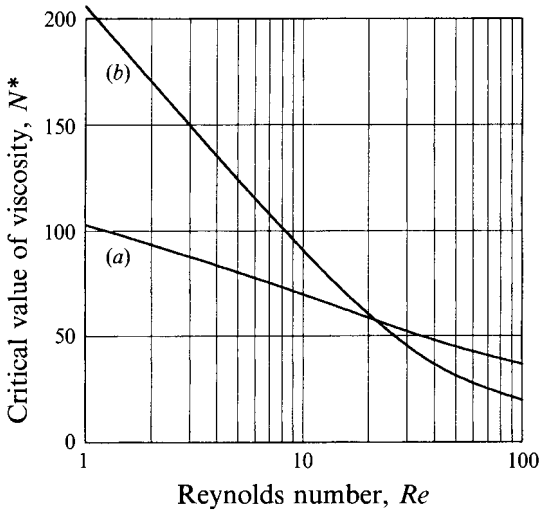

FIGURE 9. Critical value of viscosities N^* *vs.* Reynolds number. (*a*) $1/\delta = 1.1$, (*b*) $1/\delta = 1.4$.

demonstrates that the relation $G(N)$ is monotonic in character so that there always exists some critical value of N^*, above which the coefficient G is less than unity. So, N^* is the value of the viscosity ratio above which drag reduction is possible. This critical value *vs.* Reynolds number is plotted in figure 9.

4.3. *Experimental results*

For an experimental determination of the drag of a magnetic-fluid-coated cylinder a method involving the free fall of the cylinder is used. This method is most exact, and the influence of the wall of the vessel is the only complicating factor. According to the data of Stalnaker & Hussey (1979) in the case of small Reynolds numbers and a 1:10 ratio of the cylinder diameter and the distance between the walls, the drag is larger, by a factor of virtually two, than the force F_∞ in an unbounded volume, while for a 1:30 ratio it amounts to $1.25F_\infty$ (for $Re \ll 1$). This is explained by the fact that the perturbations generated by the cylinder within the flow are attenuated somewhat more slowly than, for example, would be the case for a sphere, where the effect of the walls is virtually imperceptible, even for the 1:10 ratio.

A rectangular vessel with a 15×15 cm cross-section, 40 cm in height, is used in the experiment. An elastomer with a samarium-cobalt filler is used for the preparation of the cylindrical magnet. The dimensions of two samples are 4.3 mm and 7.5 mm in diameter d_0 and 67 mm in length; the saturation magnetization of the material is 250 kA m^{-1}. A glass tube with an outer diameter of 5.6 mm for one magnet and 8.5 for the other is fitted tightly over the magnet to prevent any direct contact with the magnetic fluid, and also to maintain the cylindrical shape of the body (figure 10).

Although the presence of the vessel walls increases the drag, this addition remains a constant quantity and can be taken into consideration. The vessel is filled with silicon oil PMS-200 of viscosity $\nu_s = 1.95 \times 10^{-4}$ m^2 s^{-1}. The weight of the cylinder 5.6 mm in diameter immersed in silicon oil is $F_0 = 4.55 \times 10^{-2}$ N. The cylinder velocity is measured by a laser stop watch. A helium-neon laser beam (with a diameter of about 0.5 mm) passes through the vessel and is reflected by means of an optical-glass rectangular prism to pass once again through the vessel in the opposite direction, impinging on a photodiode. The distance between the forward and reflected laser beams is 46 mm and provides a basis for measurements. While moving the cylinder intersects the laser beam

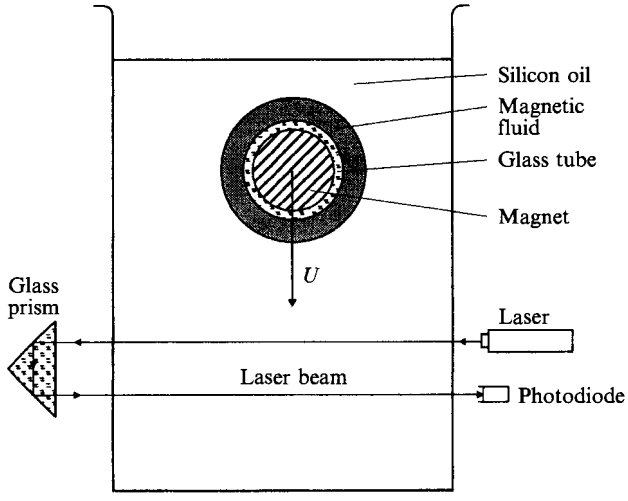

FIGURE 10. The experimental set-up.

twice. During the first intersection the photodiode signal switches on the frequency meter, while the second intersection of the beam it cuts it off. We are thus able to determine the time required to cover the base distance, i.e. the velocity at which the cylinder is moving. The measuring segment of the installation can be set at various distances from the bottom of the vessel in order to monitor the steady-state motion of the cylinder. The fluid temperature is controlled within an accuracy of 0.1 °C. In the absence of any coating, the cylinder velocity is $U_0 = 25.3$ cm s^{-1}, i.e. the Reynolds number is $Re = U_0 d_0/\nu_s = 7.28$. However, if the cylinder is moving in an infinite volume, the drag is equal to $F_\infty = C_D(Re)\rho U^2 d_0 l/2$ (l is the cylinder length), and since for $Re = 7.28$ the drag coefficient $C_D = 3.12$, then $F_\infty = 3.65 \times 10^{-2}$ N, i.e. $F_\infty/F_0 = 1.25$. Thus, although $L/d_0 = 30$ ($L = 15$ cm in the dimension of the vessel in cross-section), the drag due to the effect of the vessel walls causes an increase of 25%.

After measuring the cylinder velocity without a coating, water-based magnetic-fluid coatings are applied over the magnet in steps of 0.5 cm^3 and the velocity of the steady-state motion of the cylinder is measured again. Since the density of the magnetic fluid is $\rho_m = 1220$ kg m^{-3}, and the density of silicon oil is $\rho_s = 973$ kg m^{-3}, applying the magnetic-fluid coating increases the weight of the cylinder. Since the Reynolds number is small, the drag may be regarded as directly proportional to the cylinder velocity. With consideration of these two factors, the drag reduction $G = F/F_0$ is defined as $G = (1 + \Delta F/F_0)\, U_0/U$ where ΔF is the change in the weight of the cylinder after applying the coating; U is the cylinder velocity. The experiment is repeated for each coating thickness. The r.m.s. error in the data for each series of experiment does not exceed 0.2%. The results of the experiments are shown in figure 6 by triangles. It can be seen that the character of the experimental drag coefficient dependence on the coating thickness is quite similar to the numerical one for $Re = 10$.

The difference can be explained by two factors. First, the experimental Reynolds number is about 8 and the numerical one is equal to 10. Secondly, a more significant factor is the viscosity of the magnetic fluid. The real viscosity of a water-based magnetic fluid under a magnetic field depends in a complex fashion on the magnitude of the magnetic field and the time spent within that field. Therefore, the value of $\nu_m = 4 \times 10^{-6}$ m^2 s^{-1} measured by means of the capillary viscometer in the absence of a magnetic field, more than likely does not correspond to the viscosity of the magnetic

fluid in the coating, and $N = \nu_s/\nu_m \approx 50$ can be used only as an estimate of the viscosity ratio. Thus, we could compare the data dependence only qualitatively, not the numerical values.

In the second experiment the larger cylinder is used, with a diameter of 8.5 mm and weight $F_0 = 0.108$ N. As this cylinder without a coating falls through PMS-200 silicone oil the Reynolds number is $Re = 17.5$, which corresponds to $F_\infty = 0.0963$ N. $F_0/F_\infty = 1.12$, and this indicates a reduction in the influence of the walls as the Reynolds number increases, despite the fact that the ratio L/d_0 diminishes from 30 to 18. As in the previous case, the thickness of the coating is changed by applying magnetic fluid with a volume from 0.5 to 2.5 cm^3 in steps of 0.5 cm^3. A layer with a volume of 3 cm^3 ($\delta = 0.73$) proves to be unstable and drawn up from the cylinder by viscous flow, leaving a magnetic-fluid droplet wake. Squares identify this experiment in figure 6. Each point has been obtained by averaging the data from 10 independent measurements. The r.m.s. error in this case also does not exceed 0.2%. It can be seen that the experimental data are very close to the numerical results for $Re = 20$, $N = 100$.

5. Deformation of the magnetic-fluid coating interface by viscous flow

5.1. *Analysis for small Reynolds numbers*

It has been assumed above that the magnetic forces are stronger than the hydrodynamic ones, and the interface deformation of the magnetic-fluid coating can be neglected. However, the real relationship may be proved to be such that the interface shape will greatly differ from a circular cylinder.

A reason for deformation of the interface between the magnetic fluid and the outer flow is the difference in the hydrodynamic normal stresses over a circular surface under no magnetic field. A magnetic field altering the magnetic-fluid pressure is able to compensate for this difference. However, as the magnetostatic pressure in the magnetic field of a cylinder depends only on the radial coordinate and does not depend on the angle, such compensation of the hydrodynamic normal angle-dependent stresses requires the coating thickness to be varied with respect to the angular coordinate. Thus, a stable magnetic-fluid coating of a circular cylinder affected by a non-magnetic fluid flow must have an angular-coordinate-dependent thickness. The behaviour and the magnitude of the variation in the coating thickness, i.e. its deformation, is obviously determined by a balance of the magnetic and hydrodynamic forces and must depend on all the problem parameters: coating thickness, Reynolds number, viscosity ratio, and magnetic-to-hydrodynamic force ratio.

First, let us consider the coating deformation within the framework of Oseen's approximation adapted above for analysing the drag. With no flow a cylinder R in radius is coated with a magnetic-fluid layer, whose cylindrical surface has a radius a. When affected by the flow, the magnetic-fluid coating surface acquires a shape $r = \zeta(\theta) = a[1+f(\theta)]$ which is unknown beforehand. Assume that the deformation magnitude is much less than the layer thickness, i.e. $|f(\theta)| \ll 1-\delta$ where $\delta = R/a$. In this case, it may be considered that the interface deformation slightly alters the velocity and pressure fields. Then the latter may be denoted $\boldsymbol{v} = \boldsymbol{v}^0 + \boldsymbol{v}'$, $p = p^0 + p'$ where $\boldsymbol{v}^0$, p^0 are the velocity and pressure fields for a cylindrical coating surface shape, and their alteration due to the coating deformation obeys the inequalities $v' \ll v^0$, $p' \ll p^0$. Below, expressions (4.5) determined by Oseen's approximation will be employed for the fields of $\boldsymbol{v}^0$, p^0.

A condition for the equality of normal stresses (2.3) in a cylindrical coordinate system can be written as (surface tension is neglected)

$$\left\{-p_1+\frac{2\eta_1}{1+(\zeta'/\zeta)^2}\left[\frac{\partial v_{1r}}{\partial r}-\frac{\zeta'}{\zeta}\left(\frac{1}{\zeta}\frac{\partial v_{1r}}{\partial\theta}+\frac{\partial v_{1\theta}}{\partial r}-\frac{v_{1r}}{\zeta}\right)\right]\right\}$$

$$=\left\{\frac{2\eta_2}{1+(\zeta'/\zeta)^2}\left[\frac{\partial v_{2r}}{\partial r}-\frac{\zeta'}{\zeta}\left(\frac{1}{\zeta}\frac{\partial v_{2r}}{\partial\theta}+\frac{\partial v_{2\theta}}{\partial r}-\frac{v_{2\theta}}{\theta}\right)\right]-p_2\right\},\quad r=\zeta(\theta),\quad (5.1)$$

where $\zeta'=\mathrm{d}\zeta/\mathrm{d}\theta$. With allowance for the small magnitude of the deformation $|f(\theta)|$ and for changing velocity v' and pressure p' fields, this condition can be written at the interface $r=a$ as (accurate to the terms of the first order of infinitesimals)

$$-p_2^0(a)+2\eta_2\frac{\partial v_{2r}^0}{\partial r}+f\left[-\frac{\partial p_2}{\partial r}a+2\eta_2\frac{\partial^2 v_{2r}^0}{\partial r^2}a\right]-f'\left[\frac{\partial v_{2\theta}^0}{\partial r}-\frac{v_{2\theta}^0}{a}\right]$$

$$=-p_1^0(a)+2\eta_1\frac{\partial v_{1r}^0}{\partial r}+f\left[-\frac{\partial p_1}{\partial r}a+2\eta_1\frac{\partial^2 v_{1r}^0}{\partial r^2}a\right]-f'\left[\frac{\partial v_{1\theta}^0}{\partial r}-\frac{v_{1\theta}^0}{a}\right],\quad (r=a).\quad (5.2)$$

Equation (5.2) represents an equation with respect to f of the form

$$C_1\cos\theta+(C_2+C_3\cos\theta)f-f'C_4\sin\theta=0,\quad (5.3)$$

where the constants C_1, C_3, C_4 are determined by the fields of $\boldsymbol{v}^0$, p^0, and the constant C_2 depends on the hydrostatic pressure $\mathrm{d}p_M/\mathrm{d}r$ alone. It is natural to suppose that the magnetic forces are predominant for small surface deformations, i.e. the relation $C_2\gg C_1$, C_3, C_4 is valid. The validity of this supposition will be evaluated below, proceeding from the solution found and the explicit form of the quantity $\mathrm{d}p_M/\mathrm{d}r$. Then equation (5.3) reduces to the form $f(\theta)=C_1\cos\theta/C_2$, i.e. the deformed surface is governed by the expression

$$f(\theta)=-\frac{1}{a}\left[p_2^0-p_1^0+2\eta_1\frac{\partial v_{1r}^0}{\partial r}-2\eta_2\frac{\partial v_{2r}^0}{\partial r}\right]\left(\frac{\mathrm{d}p_M}{\mathrm{d}r}\right)^{-1},\quad (r=a).\quad (5.4)$$

With the explicit form of expressions (4.5) for the velocity and pressure taken into account, (5.4) can be written

$$f(\theta)=-\frac{\eta_1 U}{a^2}\left(-\frac{\mathrm{d}p_M}{\mathrm{d}r}\right)_{r=a}^{-1}f_0(\delta)\cos\theta,\quad (5.5)$$

where the function $f_0(\delta)$ is of the form

$$f_0(\delta)=\frac{\delta^4-12\delta^2-13-4\delta^2\ln\delta(7-4\ln\delta)}{\frac{1}{2}[\ln(\gamma Re/8\delta)-1]FN+\frac{1}{2}A[2\ln(\gamma Re/8\delta)-1]}.\quad (5.6)$$

Thus, the results obtained for the small-deformation approximation and restricted to low Reynolds numbers show that the deformation surface represents a circular cylinder, as before, but shifted by the flow relative to the solid cylinder. The magnitude of this shift appears directly proportional to the fluid viscosity and flow velocity and inversely proportional to the magnetic field non-uniformity.

The magnetic field of a live current conductor ($H=I/2\pi r$) is not large, and in this case the linear magnetization law ($M=\chi H$) may be utilized. Then the magnetostatic pressure gradient is equal to

$$\left(-\frac{\mathrm{d}p_M}{\mathrm{d}r}\right)_{r=a}=-\frac{1}{2}\frac{\mathrm{d}}{\mathrm{d}r}(\mu_0\chi H^2)=4\mu_0\chi\pi^2I^2\frac{\delta^3}{R^3}$$

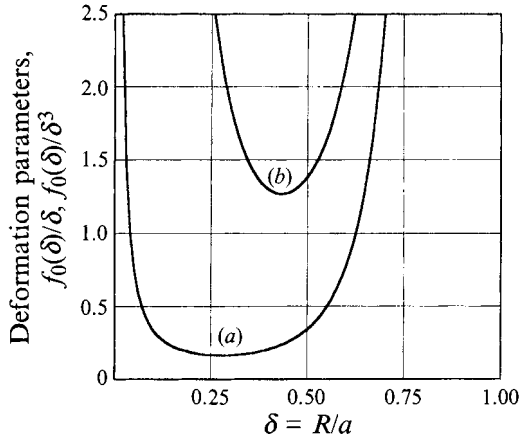

FIGURE 11. Dependence of deformation magnitude on coating thickness. (*a*) $f_0(\delta)/\delta$, (*b*) $f_0(\delta)/\delta^3$.

and the magnitude of the interface deformation is described by the expression

$$f(\theta) = \epsilon_I \frac{f_0(\delta)}{\delta} \cos\theta,$$

where $\epsilon_I = 4\eta_1 UR\pi^2/\mu_0 \chi I^2$. A similar expression governs the function $f(\theta)$ in the case of a strongly magnetized cylinder, except that the proportionality factor has the form $\epsilon_M = \eta_2 U/\mu_0 M_S M_I R$ where M_S is the saturation magnetization of the magnetic fluid. If the cylinder is magnetized weakly, then the surface deformation depends on the coating thickness in the following fashion:

$$f(\theta) = \epsilon_\chi \frac{f_0(\delta)}{\delta^3} \cos\theta,$$

where $\epsilon_\chi = \eta_1 U/\mu_0 \chi M_I^2 R$.

Figure 11 plots the behaviour of the function $f_0(\delta)/\delta$ (curve *a*) and $f_0(\delta)/\delta^3$ (curve *b*) *vs.* coating thickness for $N = 240$, $Re = 0.03$. It is seen that the deformation magnitude grows sharply at small ($\delta \to 1$) and large ($\delta \to 0$) magnetic-fluid layer thicknesses. This takes place because for small coating thicknesses the circulation flow in a magnetic-fluid layer can occur only at large pressure drops, i.e. at a high surface deformation. For large coating thicknesses the pressure gradient necessary to give rise to circulation flow decreases but the magnetic field gradient holding the coating diminishes still more strongly. Thus, from the viewpoint of providing magnetic-fluid coating stability, i.e. the minimal interface deformation subjected to the external flow, the coating thickness $\delta \approx 0.5$ is optimal. As seen from figure 11, the deformation is minimum over this coating thickness range.

5.2. *Analysis for moderate Reynolds numbers*

An analytical study has allowed us only to reveal the general behaviour of the coating shape when affected by the flow but not to establish quantitative data because it is restricted to small Reynolds numbers and low deformation of the coating. The most interesting question is the mutual interaction between the fluid flow structure and shape of the coating interface. Such mutual interaction can be studied only in a full problem statement. The flow structure and coating shape must be defined simultaneously. But here we run into a limited choice of analytical and numerical methods for such a kind of problem.

Kamiyama & Satoh (1988) have analysed this problem numerically, using the small-parameter method and restricting to a small coating thickness and small deformation. Now we are studying this problem without any restrictions.

The formulation of the interface conditions is the main difference between the analysis of flow past an arbitrary coating and a cylindrical one. Now condition (4.9) must be written as

$$\frac{\partial \psi_1}{\partial n} = \frac{\partial \psi_2}{\partial n} = v_\tau, \tag{5.7}$$

where the coordinate n is normal to the surface, and condition (4.10) assumes the form

$$N(\omega_1 + 2kv_\tau) = (\omega_2 + 2kv_\tau), \tag{5.8}$$

where the coordinate τ is tangential to the interface, v_τ is the velocity at the interface, and k is its curvature. Conditions (5.7) and (5.8) permit numerical boundary conditions to be used for determining the vorticity on both sides of the interface. These boundary conditions are detailed in Kamiyama & Krakov (1993).

Also, the normal stress equality condition (2.3) must be satisfied at the interface and can be reduced to the form (with constant surface tension coefficient $\partial\alpha/\partial\tau = 0$)

$$W\left[\left(\frac{1}{Ro} - 1\right)\frac{Re}{2}\frac{\partial v_\tau^2}{\partial \tau} + 2\frac{N-1}{N}k(\omega_i - kv_\tau)\right] - \frac{\mathrm{d}k}{\mathrm{d}\tau} = Bo_m \frac{\partial p_M}{\partial \tau}, \tag{5.9}$$

where $W = \eta_1 U/\alpha$ is the Weber number, $Bo_m = \mu_0 M |\nabla H| a^2/\alpha$ is the magnetic Bond number, ω_i is equal to ω_1 or ω_2 depending on surface curvature: at a surface point where the interface is convex ($k < 0$) $\omega_i = \omega_1$; at a surface point where the interface is concave ($k > 0$) $\omega_i = \omega_2$.

The right-hand side of (5.9) can be written in a polar coordinate system with respect to a cylinder in the form

$$Bo_m \frac{\partial p_M}{\partial \tau} = Bo_m \frac{\partial p_M}{\partial r} \frac{\zeta'/\zeta}{[1 + (\zeta'/\zeta)^2]^{1/2}}, \tag{5.10}$$

where $r = \zeta(\theta)$ is the equation for the interface, and $\zeta' \equiv \mathrm{d}\zeta/\mathrm{d}\theta$.

Relation (5.9) can be considered as a first-order differential equation with respect to the surface $\zeta(\theta)$, if its left-hand side is assumed to be constant. This has been used to solve the problem numerically. In addition, as has been mentioned above, for a magnetized cylinder the characteristic values of the Bond number at the coating surface are of the order of 1000. W has the order of unity, and the term $\mathrm{d}k/\mathrm{d}\tau$ in (5.9) is of order of 10^{-3}. Therefore, in this analysis this term has hardly any influence on the calculation results, and the ratio of Weber number to magnetic Bond number $W_c = W/Bo_m$ has been used as a characteristic parameter.

The following approach is used. First, the problem is solved for a given interface (at the first step with $r = a$) under boundary conditions (5.7) and (5.8). Then, equation (5.9) yields a new interface: the left-hand side of equation (5.9) is determined in terms of preliminarily calculated values of v_τ, ω and is considered constant. In this case, (5.9), with its right-hand side in the form of (5.10), is the first-order differential equation for ζ.

Upon solving this equation for a fixed volume of coating and defining a new position of the interface, the grid is reconstructed according to the scheme described above, to find the interface. Equations of motion (4.7) and (4.8) are again solved for a new interface. To determine ζ the procedure is repeated until the interface $\zeta(\theta)$ ceases to vary.

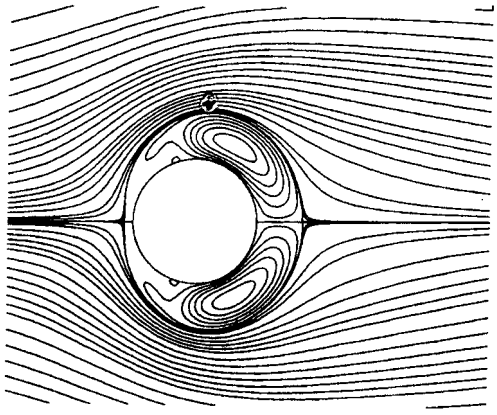

FIGURE 12. Flow structure and shape of the interface pattern for $Re = 10$, $1/\delta = 1.6$, $N = 100$, $W_c = 0.003$.

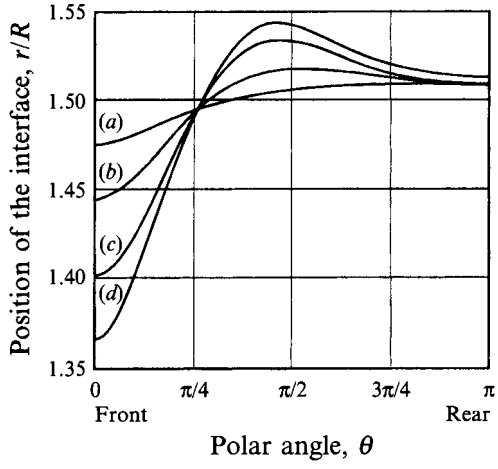

FIGURE 13. Change of the interface shape with Reynolds number for $W_c = 1.75 \times 10^{-3}$, $1/\delta = 1.5$, $N = 1$. (*a*) $Re = 1$; (*b*) $Re = 7$; (*c*) $Re = 20$; (*d*) $Re = 30$.

A numerical study is done using the same grid as in the case of the non-deformed interface (5751 nodes) but the grid has been adapted to the interface. The system of algebraic equations has been solved by Gauss–Seidel's iteration method within an accuracy of 5×10^{-6}. Runge–Kutta's method is used to determine an interface shape from equation (5.9), with its right-hand side in the form of (5.10). The solution obtained is approximated by cubic splines.

The flow structure and magnetic-fluid-coating surface shape for $Re = 10$, $\delta = 1.6$, $N = 100$, $W_c = W/Bo_m = 0.003$ are shown in figure 12. As the magnetic fluid viscosity is small ($N = 100$), there is no flow separation in the external flow but the flow structure in the coating is intricate in nature, and even a small recirculation flow region is observed. In this case, the coating is oblate: in cross-section it has a markedly larger size to the rear. The coating has the minimum thickness in the region of the forward stagnation point.

It is obvious that the surface deformation must depend on the flow structure. As it is easier to obtain flow structure differences at magnetic fluid viscosity values that are not too small, the case $N = 1$ has been analysed. Figure 13 shows the coating shape for

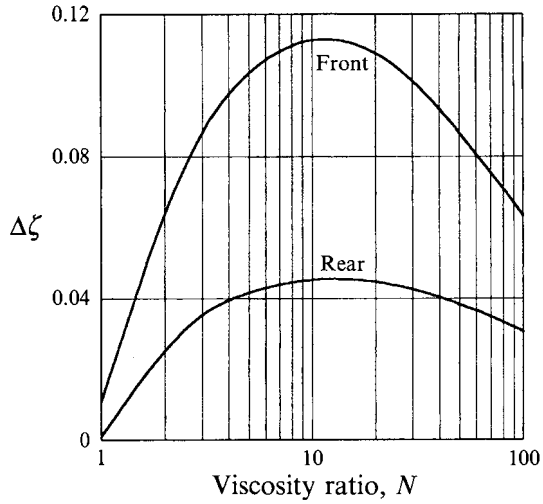

FIGURE 14. Deformation of the interface at the front and rear critical points versus the ratio of non-magnetic to magnetic fluid viscosity. $Re = 10$, $1/\delta = 1.25$, $W_c = 1 \times 10^{-4}$.

different Reynolds numbers with $N = 1$. It is seen that for $Re = 1$ the coating shape does not greatly differ from the sinusoidal one obtained in the course of the analytical study. This is supported by the conclusion that at small Reynolds numbers when flow behind a cylinder and in front of it is close to symmetrical the coating is shifted as a whole unit relative to the solid cylinder, hardly modifying its shape. As the Reynolds number increases, the flow loses its symmetry, the recirculation flow region appears, and the coating in the region of the rear stagnation point becomes thinner, acquiring a shape similar to the one in figure 12 (figure 13, curve *d*).

It is clear that as the magnetic fluid viscosity also determines the flow structure and pressure distribution along the coating surface, it is one of the main factors responsible for the coating deformation magnitude. For a fixed value of the Reynolds number the magnetic-fluid viscosity variation alters the parameter N only. It has been found that the relationship between the coating deformation magnitude and magnetic-fluid viscosity is non-monotonic in nature. The quantity $\Delta\zeta = |\zeta(\theta) - a|$ calculated at the forward and rear stagnation points has been taken as a quantitative measure of the coating deformation magnitude. From figure 14 it is seen that for small and large magnetic-fluid viscosities the deformation magnitude noticeably falls. Apparently, this may be attributed to the two-fold effect of this viscosity on coating deformation. On the one hand, decreasing the magnetic-fluid viscosity η_2 reduces the pressure drop inside the coating and, hence, the deformation. But, on the other hand, the decrease gives rise to a surface velocity v_r, thereby augmenting the coating deformation. The balance of these two mechanisms specifies the resultant deformation. As seen from figure 14, there is a maximum for $N \sim 10$.

Coating deformation also grows with increasing flow velocity, i.e Reynolds number (figure 15). The results obtained show that in the non-separated flow region ($Re < 10$) the relation $\Delta\zeta(Re)$ is linear. At large Re when the flow asymmetry ahead of and behind the cylinder increases, the deformation degree grows sharply with increasing Re.

A magnetic field is the only force keeping the coating on the cylinder surface. When the field falls off with parameter W_c, coating deformation under the action of the flow naturally increases. From figure 16 it is seen that the relation $\Delta\zeta(W_c)$ is practically linear. This is expected, as coating deformation only slightly alters the external flow

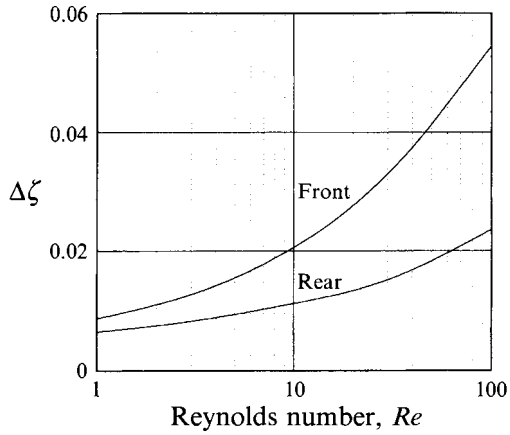

FIGURE 15. Influence of Reynolds number on the interface deformation. $N = 100$, $1/\delta = 1.4$, $W_c = 1 \times 10^{-3}$.

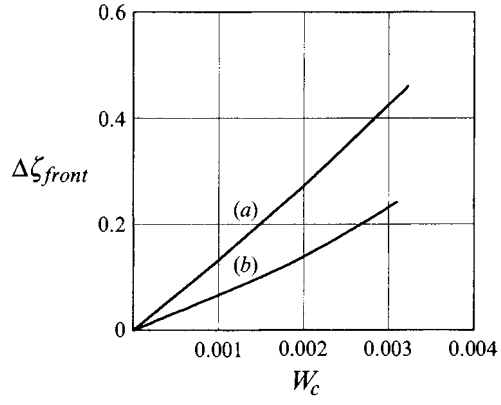

FIGURE 16. Deformation at the front critical point *vs.* W_c. $Re = 10$, $N = 100$. (*a*) $1/\delta = 1.6$, (*b*) $1/\delta = 1.4$.

structure, i.e. the hydrodynamic effect on the coating hardly changes, and the deformation magnitude is practically determined by the W/Bo_m ratio alone, i.e. W_c. This means that the relation $\Delta\zeta(W_c)$ must be almost linear in nature. Possibly, the behaviour of the relation changes as $\Delta\zeta_{front} \to 1/\delta - 1$, i.e. as the coating thickness decreases at the forward stagnation point to zero. However, in the course of the numerical analysis no corresponding results have been obtained: for $\delta - 1 - \Delta\zeta_{front} < 0.1$ the iteration process diverged. It is difficult to point uniquely to whether the reason for the divergence is numerical or physical in nature: in the course of the above-described experiment the coating was blown off by the flow before the coating thickness at the forward stagnation point becomes equal to zero. Therefore, it may be assumed that the numerical instability at small thicknesses has a physical nature.

6. Conclusion

The method of modifying viscous fluid flow structure over a solid body by coating it with a layer of magnetic fluid is investigated analytically, numerically and experimentally. It is discovered that a magnetic-fluid coating could prevent flow

separation and lead to drag reduction. These effects are possible if the viscosity of the magnetic fluid is less than the viscosity of the outer fluid. The analysis of the shape of the coating interface shows that a magnetic-fluid coating could be effectively established by the magnetic field of the solid.

The method studied could be used for modifying flow structure, leading to drag reduction in flows of highly viscous fluids such as oil or chemical products. The magnetic fluid does not have to be soluble in the outer fluid.

REFERENCES

BASHTOVOI, V. G., BERKOVSKY, B. M. & VISLOVICH, A. N. 1988 *Introduction to Thermomechanics of Magnetic Fluids*. Hemisphere.

BASHTOVOI, V. G. & KRAKOV, M. S. 1978 Stability of an axisymmetric jet of magnetizable fluid. *Appl. Math. Tekhn. Phys.* (in Russian), no. 4, 147–153.

BERKOVSKY, B. M., MEDVEDEV, V. F. & KRAKOV, M. S. 1993 *Magnetic Fluids – Engineering Applications*. Oxford University Press.

COWLEY, M. D. & ROSENSWEIG, R. E. 1967 The interfacial stability of a ferromagnetic fluid. *J. Fluid Mech.* **30**, 671–688.

DENNIS, S. C. R. & CHANG, G.-Z. 1970 Numerical solutions for steady flow past a circular cylinder at Reynolds number up to 100. *J. Fluid Mech.* **42**, 471–489.

FORNBERG, B. 1980 A numerical study of steady viscous flow past a circular cylinder. *J. Fluid Mech.* **98**, 819–855.

ISAAK, J. D. & SPEED, B. 1906 *Engng News* **55**, 641.

KAMIYAMA, S. & KRAKOV, M. S. 1993 Numerical simulation of steady flow around a circular cylinder coated with magnetic fluid. *Proc. Intl Symp. on Aerospace and Fluid Science, Sendai, Japan*, vol. II, pp. 705–712. Japan Society of Comput. Fluid Dynamics.

KAMIYAMA, S. & SATOH, A. 1988 Steady flow around a cylinder coated with a magnetic fluid film. *JSME Intl J.* (II) **31**, 218–226.

KAMIYAMA, S. & SHIMOIIZAKA, J. 1985 Magnetic fluids and their applications. *J. Japan Soc. Mech. Engrs* (in Japanese) **88**, 596–602.

KRAKOV, M. S. 1992 Control volume finite-element method for Navier-Stokes equation in vortex–streamfunction formulation. *Numer. Heat Transfer* B: *Fundam.* **21**, 125–145.

LAMB, H. 1932 *Hydrodynamics*. Cambridge University Press.

LANDAU, L. D., LIFSHITZ, E. M. & PITAEVSKII, L. P. 1984 *Electrodynamics of Continuous Media*. Pergamon.

NEURINGER, J. L. & ROSENSWEIG, R. E. 1964 Ferrohydrodynamics. *Phys. Fluids* **7**, 1927–1937.

POLEVIKOV, V. K. 1986 A numerical study of drag of a circular cylinder coated by thin magnetic fluid layer. *Fluid Dyn.* (in Russian) no. 3, 11–16.

RAYLEIGH 1878 On the instability of jets. *Proc. Lond. Math. Soc.* **10**, 4.

ROSENSWEIG, R. E. 1985 *Ferrohydrodynamics*. Cambridge University Press.

STALNAKER, F. & HUSSEY, R. G. 1979 Wall effects on cylinder drag at low Reynolds number. *Phys. Fluids* **22**, 603–613.

TAKAMI, H. & KELLER, H. B. 1969 Steady two-dimensional viscous flow of an incompressible fluid past a circular cylinder. *Phys. Fluids* **12**, Suppl. II, 51–56.